17th World Conference on Earthquake Engineering, 17WCEE
Sendai, Japan - September 13th to 18th 2020

KINEMATIC SOURCE MODELING FOR PREDICTED GROUND MOTION BY DYNAMIC RUPTURE SIMULATION

M. Yamada [1], K. Hada [2], Y. Fujino [3], R. Imai [4], K. Takamuku [5], H. Fujiwara [6]

[1] *Ph.D., NEWJEC Inc., yamadams@newjec.co.jp*
[2] *Ph.D., NEWJEC Inc., hadakj@newjec.co.jp*
[3] *NEWJEC Inc., fujinoys@newjec.co.jp*
[4] *Ph.D., Mizuho Information & Research Institute, Inc., ryuta.imai@mizuho-ir.co.jp*
[5] *Mizuho Information & Research Institute, Inc., kei.takamuku@mizuho-ir.co.jp*
[6] *Ph.D., National Research Institute for Earth Science and Disaster Resilience, fujiwara@bosai.go.jp*

Abstract

The dynamic fault rupture simulation was conducted using the three dimensional finite difference method without giving a priori rupture starting area and rupture stopping area by changing the coefficient of friction or changing the frictional constitutive law. It was conducted on condition that the shear rigidity was changed along the fault plane and that the shear stress on the fault plane was loaded by forced displacement.

A rectangular parallelepiped model was prepared with 60km long for x-direction which was strike direction of the fault plane, 20km long for y-direction which was orthogonal to strike direction of the fault plane and 8km high for vertical direction z. The model was assumed horizontal layered structure with 4 layers and thickness of each layer was 2km. The first layer was surface layer (layer above the upper end of the fault plane layer), the second layer was the fault plane layer, the third layer was the lower from the bottom of the seismogenic layer and the fourth layer was the transition layer to the viscous boundary of the bottom of the model which didn't dislocate.

The top of the model was the stress-free boundary, and the bottom and the edge for x-direction were the viscous boundary condition. The forced displacement was given at the edge for y-direction and induced the shear stress in the model body. For the second layer of the fault plane layer, the 20% higher shear wave velocity was given at central part for x-direction of x=-0.5km～x=+0.5km than the velocity for standard bedrock such as neighbor parts. And the induced shear stress by the displacement at the central part was larger than other parts. Fault rupture was occurred spontaneously from the central part in spite that the static friction coefficient was set constant in each layer.

On the other hand, the 20% lower shear wave velocity was given at outskirts part for x-direction of x＞±5.0km for the fault plane layer. The fault rupture started at the central part was spontaneously stopped after approximately around 10km spread in the direction of the plus and minus of x, because the induced shear stress by the displacement at the part was smaller.

They were consistent with previous studies in the fault rupture process that the stress drop was about 2MPa and that the rupture velocity was 3～3.5km/s at most. We estimated the near fault ground motion for our model fault by using this dynamic rupture simulation.

Kinematic source models were prepared referring to the dynamic fault rupture simulation. The predicted ground motions by statistical Green's function method were compared with the motion predicted by the dynamic simulation. Y-component ground velocity was especially large around x=±5～10km for the model with SMGA locating at the boundary of media. This feature coincided with the result of the dynamic simulation. This coincidence implied that the SMGA did not necessarily correspond to the large slip area.

Keywords: dynamic fault rupture simulation, ground motion, forward modeling, kinematic source parameter

1. Introduction

In recent years, the dynamic fault rupture simulation is used widely for the solution of the physical phenomenon of the fault dislocation and so on.

Tsuda (2016) [1] tried to reproduce the rupture process of mega-thrust earthquakes such as the 2011 off the Pacific coast of Tohoku Earthquake. Kase (2016) [2] tried to explain the source process of the intersegmental rupture propagation for the 2014 northern Nagano earthquake. Kase et al. (2002) [3] simulated the earthquake rupture process on the Uemachi fault system. Irie (2014) [4] explored to be clear for the source properties of large inland strike-slip faults for strong motion prediction based on dynamic rupture simulation. However, in these simulations, the initial rupture area that was given smaller static friction coefficient and the rupture stop area in which rupture was not permitted were indispensable.

Kame (1997) [5] developed the calculation method of the analysis of spontaneous rupture growth with geometrical complexity. But it was different from our study that Kame (1997) [5] assumed an initial fault plane having a length of critical crack.

In this study, the dynamic fault rupture simulation was conducted without giving a priori rupture starting area and rupture stopping area by changing the coefficient of friction or changing the frictional constitutive law. It was conducted on condition that the shear rigidity was changed along the fault plane and that the shear stress on the fault plane was loaded by forced displacement. Kinematic source models were prepared to refer to the dynamic fault rupture simulation. The predicted ground motions by Statistical Green's function method were compared with the motion predicted by the dynamic simulation.

2. Procedure and condition of the dynamic fault rupture simulation

2.1 Simulation model

Three-dimensional finite difference method (Kase 2010) [6] was used for the dynamic fault rupture simulation.

A rectangular parallelepiped model was prepared with 60km long for x-direction, which was strike direction of the fault plane, 20km long for y-direction, which was orthogonal to strike direction of the fault plane and 8km high for vertical direction z. The model was assumed horizontal layered structure with 4 layers and thickness of each layer was 2km. The second layer was the fault plane layer. The first layer was surface layer above the upper end of the fault plane layer. The third layer was the lower from the bottom of the seismogenic layer. The fourth layer was the transition layer to the viscous boundary of the bottom of the model which didn't dislocate. Simulation model section (x-z section) is shown in Fig. 1. Rupture is not permitted in gray shaded areas.

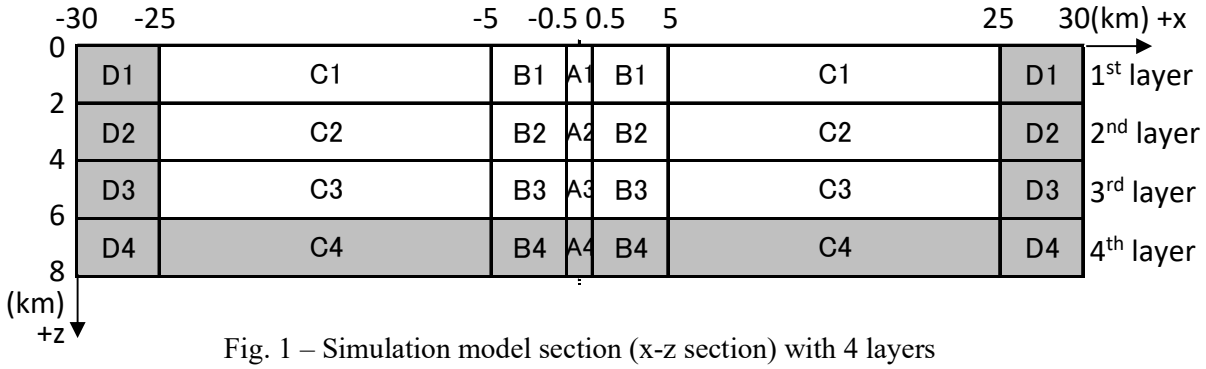

Fig. 1 – Simulation model section (x-z section) with 4 layers

2.2 Boundary condition and simulation model properties

The top of the model was the stress-free boundary, and the bottom and the both edge of x-direction were the viscous boundary condition. The forced shear displacement was given at the edge of y-direction and induced the shear stress in the model body.

For the second layer of the fault plane layer, the 20% higher shear wave velocity was given at central part "A2" of x=-0.5km～x=+0.5km than the velocity for standard bedrock such as neighbor parts "B2". The induced shear stress by the displacement at the central part was larger than other parts. On the other hand, the 20% lower shear wave velocity was given at outskirts part "C2" of x＞±5.0km for the fault plane layer. The static friction coefficient was set constant in each layer. Detailed model properties for each area were shown in Table 1. Rupture is not permitted in gray shaded areas.

Table 1 –Simulation model properties for each area

Layer	Area	V_p (km/s)	V_s (km/s)	ρ (t/m^3)	μ_s	μ_d	D_c (m)	Rupture
1st surface	A1	2.100	0.700	2.00	0.02	0.0	4.58	permitted
	B1	2.100	0.700	2.00	0.02	0.0	4.58	
	C1	2.100	0.700	2.00	0.02	0.0	4.58	
	D1	2.100	0.700	2.00	1	0.0	4.58	not permitted
2nd fault	A2	7.200	4.157	2.67	0.0364	0.0	0.10	permitted
	B2	6.000	3.464	2.67	0.0364	0.0	0.14	
	C2	4.800	2.771	2.67	0.0364	0.0	0.22	
	D2	4.800	2.771	2.67	1	0.0	0.22	not permitted
3nd under fault	A3	7.000	4.000	2.90	0.2	0.0	0.10	permitted
	B3	7.000	4.000	2.90	0.2	0.0	0.10	
	C3	7.000	4.000	2.90	0.2	0.0	0.10	
	D3	7.000	4.000	2.90	1	0.0	0.10	not permitted
4th transition for boundary	A4	7.000	4.000	2.90	1	0.0	0.10	not permitted
	B4	7.000	4.000	2.90	1	0.0	0.10	
	C4	7.000	4.000	2.90	1	0.0	0.10	
	D4	7.000	4.000	2.90	1	0.0	0.10	

3. Result of the dynamic fault rupture simulation

3.1 Share stress before rupture start

Fig. 2 shows spatial distribution of share stress be-fore rupture start. It was found that the stable shear stress of the central part induced by the forced dis-placement was larger because higher shear wave velocity was given for this area.

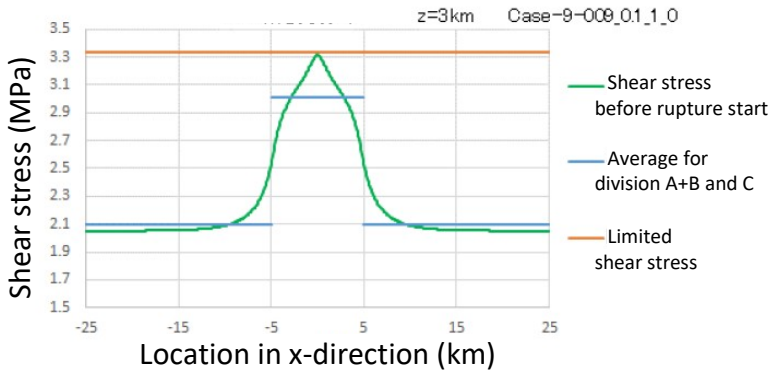

Fig. 2 – Spatial distribution of share stress before rupture start

3.2 Share stress after rupture start

Fig. 3 shows spatial distribution of share stress after rupture start. Spontaneous fault rupture was occurred from the central part, although the static friction coefficient was set constant in this layer. The fault rupture starting at the central part was spontaneously stopped after the rupture spread at around 10km in the x-direction. It caused that the induced shear stress by the displacement at the part was smaller because the lower shear wave velocity was given at the corresponding outskirts part for the fault plane layer. In this figure, the stress drop was about 2MPa.

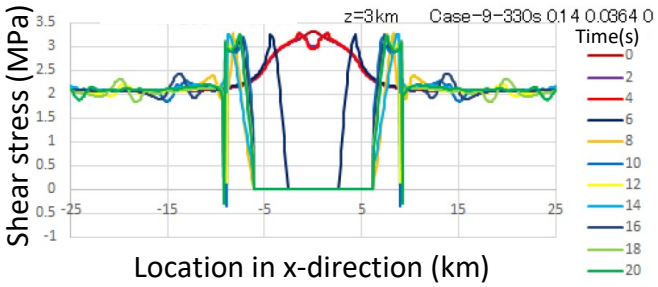

Fig. 3 –Spatial distribution of share stress after rupture start

Fig. 4 shows distribution of rupture time in x-direction. Fig. 5 shows snap shots of x-component dislocation for x-y section at the depth of z=3km from 5s to 10s after rupture start. Fig. 6 shows distribution of rupture time on the fault plane. It was found that the spontaneous fault rupture started at the central part was stopped after the rupture spread at around 10km in the x-direction as same as shown in Fig. 3.

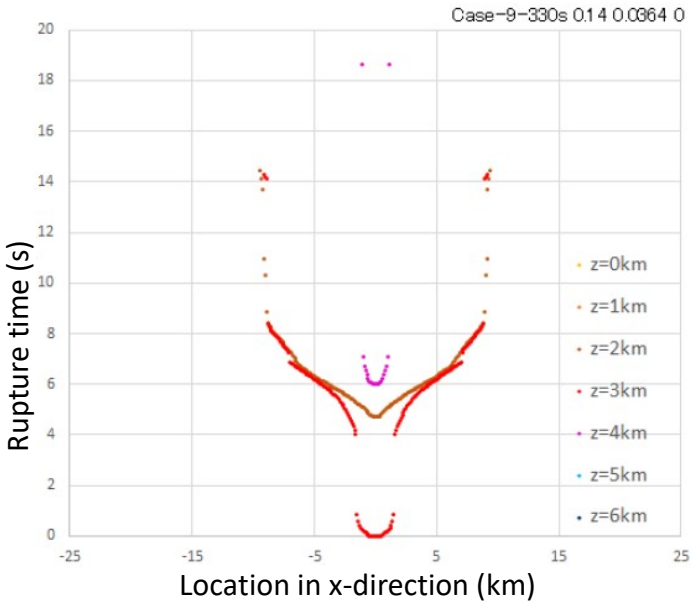

Fig. 4 –Distribution of rupture time in x-direction

3.3 Rupture velocity

Fig. 7 shows distribution of rupture velocity on the fault plane. After rupture starts, the rupture velocity got faster up to 3-3.5km/s at around x=±4～7km while propagating and drastically slowed down to stop at x=±9km.

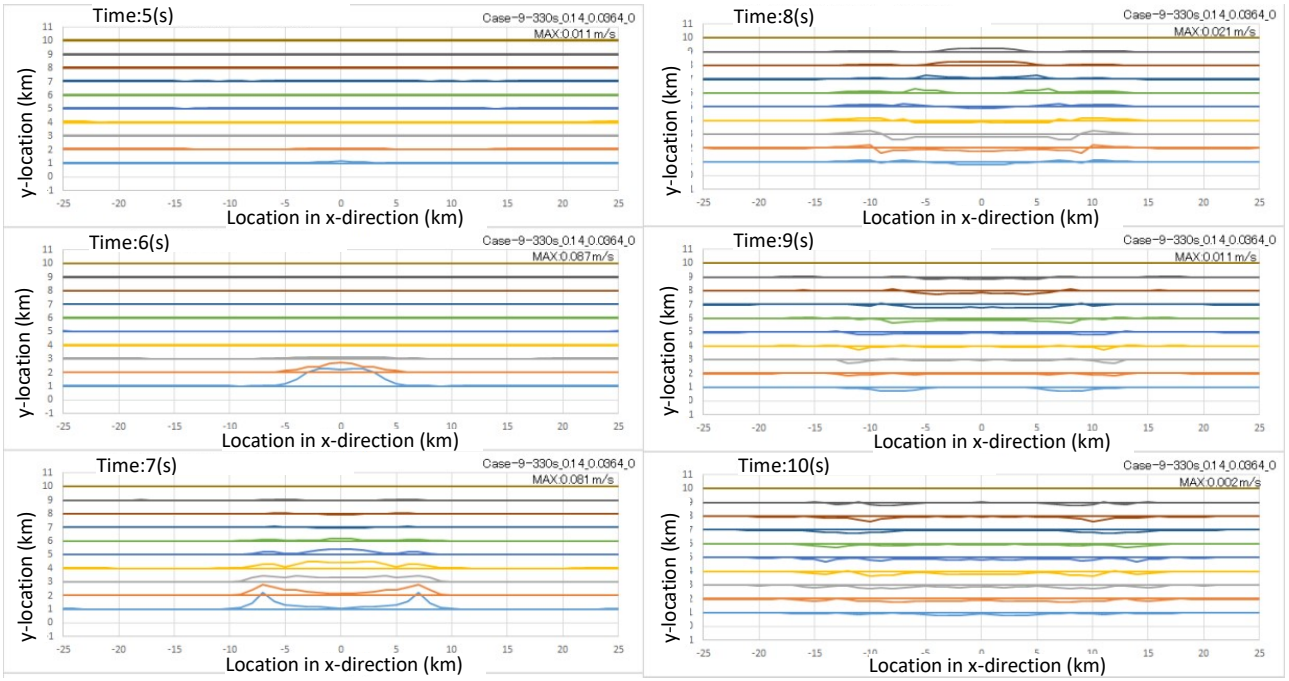

Fig. 5 – Snap shots of dislocation for x-direction at the depth of z=3km from 5s to 11s after rupture start

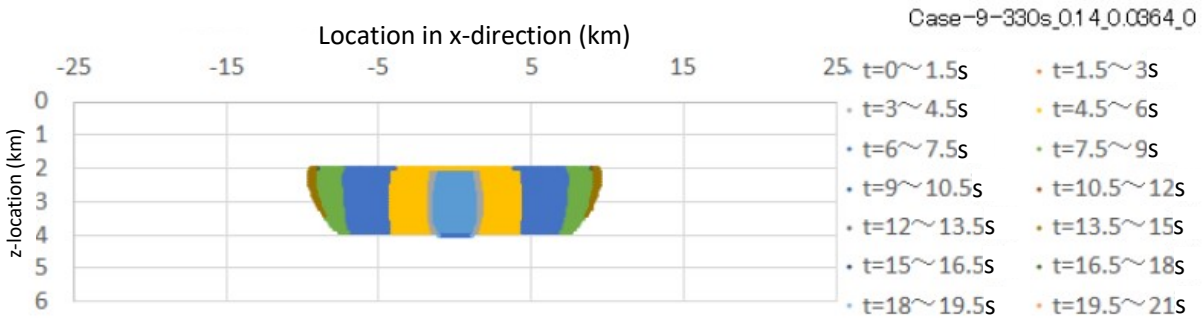

Fig. 6 – Distribution of rupture time on the fault plane

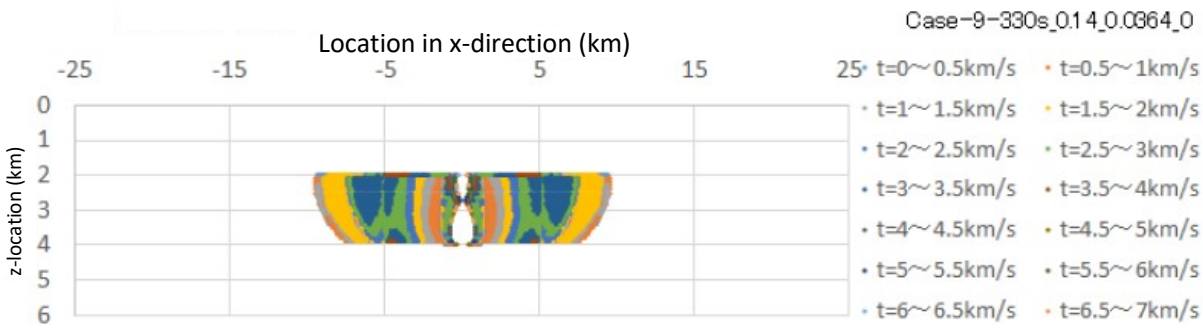

Fig. 7 –Distribution of rupture velocity on the fault plane

3.4 Ground motion near the fault line

Fig. 8 shows velocity waveform on ground surface (z=0km) at 0.1km in y-direction apart from the fault line. Y-component of ground motion was larger than x-component of ground motion because rupture was not propagated to the 1st layer. Y-component of ground velocity was especially large at around x=±5～10km.

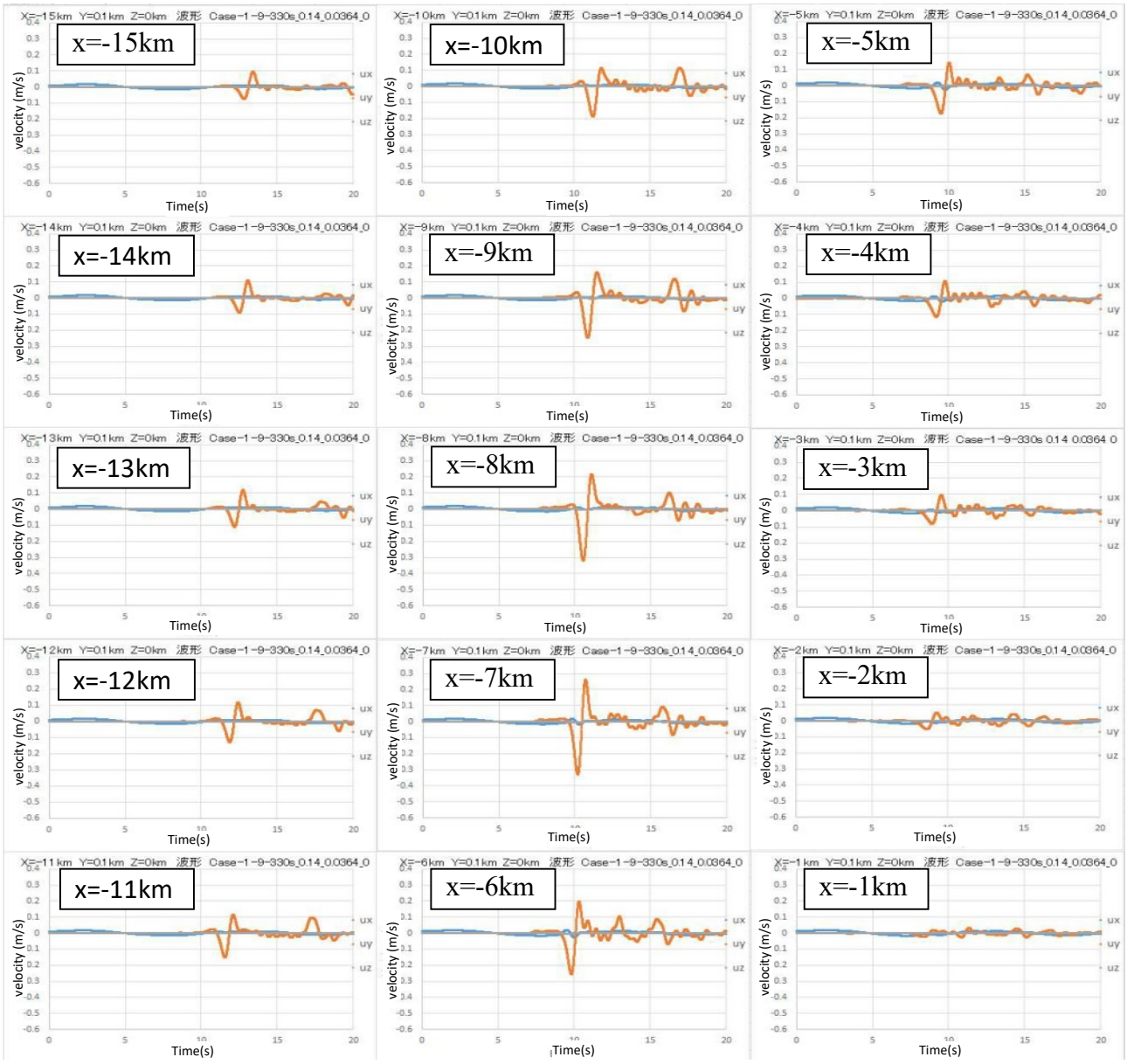

Fig. 8 –Velocity waveform on ground surface (z=0km) at 0.1km apart from the fault line for y-direction

3.5 Slip on the fault plane

Fig. 9 shows time history of slip on the fault plane at each location in the x-direction. Fig. 10 shows distribution of slip on the fault plane in the x-direction. It was found that the slip on the fault plane was about 0.25m at the center part between x=-5km and x=+5km in the x-direction.

3.6 Slip velocity

Fig. 11 shows comparison of slip velocity time function between by this study and by Nakamura & Miyatake (2000). In Fig. 11, the slip velocity time function by this study was directly calculated at the points of (x,y,z)=(3,0,3) and (5.5,0,3) by the dynamic fault rupture simulation. The slip velocity time function by Nakamura & Miyatake (2000)[7] was estimated by using rupture velocity, stress drop and slip that was obtained by the simulation of this study at the same points. The point of (x,y,z)=(3,0,3) was corresponding to strong motion generation area (SMGA), both slip velocity time functions were reasonably coincided each other. The point (x,y,z)=(5.5,0,3) was not corresponding to SMGA, slip velocity time function by this study

was similar to that by Nakamura & Miyatake (2000)[7] in its shape but was smaller in its peak slip velocity than that.

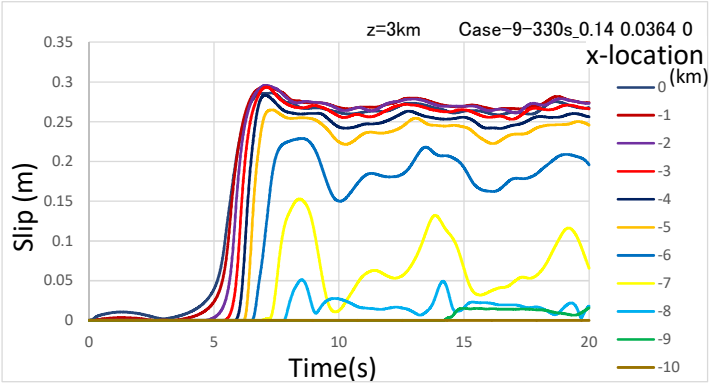

Fig. 9 –Time history of slip on the fault plane at each location in the x-direction

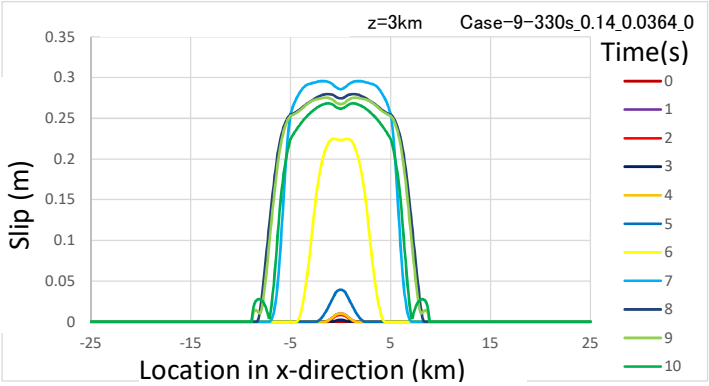

Fig. 10 –Distribution of slip on the fault plane in the x-direction

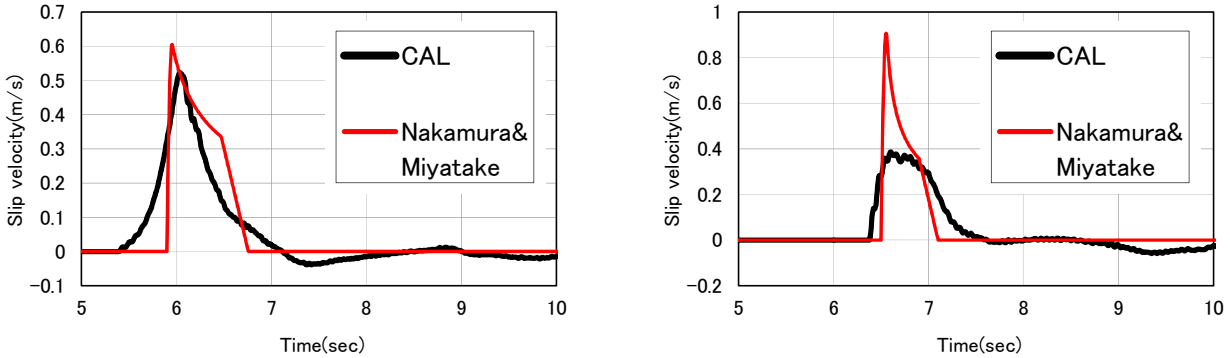

(a) Point (x,y,z)=(3,0,3) (km) (b) Point (x,y,z)=(5.5,0,3) (km)

Fig. 11 –Comparison of slip velocity time function between by this study and Nakamura & Miyatake (2000)

4. Ground motion prediction by statistical Green's function method

Two kinematic source models were prepared referring to the dynamic fault rupture simulation mentioned previously. Ground motions were predicted on ground surface (z=0km) at 0.1km in y-direction apart from the fault line by statistical Green's function method.

4.1 Kinematic source models

One kinematic source model shown in Fig. 12(1) had the SMGA locating at the center of the fault where large slip in the x-direction was distributed in the dynamic fault rupture simulation shown in Fig. 10. Another model shown in Fig. 12(2) had the SMGA locating at the boundary of media where high rupture velocity was distributed in the dynamic simulation shown in Fig. 7.

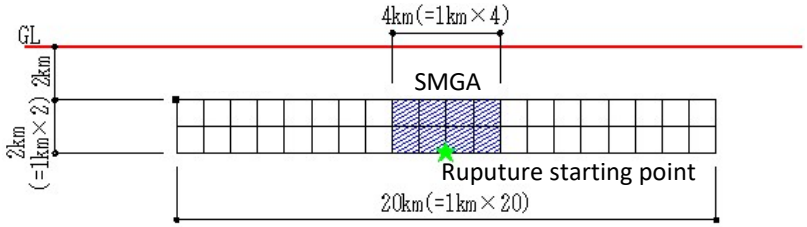

(1) Source model with SMGA locating at the center of the fault

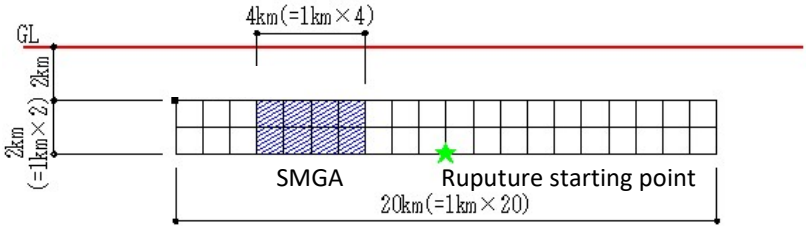

(2) Source model with SMGA locating at the boundary of media

Fig. 12 –Kinematic source models

Table 2 –Kinematic source parameter

Fault	Length	km	20
	Width	km	2
	Area(S)	km^2	40
	Seismic moment($M_0=\mu DS$)	dyne・cm	3.20E+24
	Density(ρ)	g/cm^3	2.67
	Shear wave velocity(Vs)	km/s	3.464
	Rigidity(μ)	$g/cm・s^2$	3.20E+11
	Average slip(D)	cm	25.0
	Rupture velocity(Vr)	km/s	2.5
	Rise time(tr)	sec	0.30
SMGA	Area of fault covered by SMGA		0.22
	Average SMGA slip contrast		2
	Area(Sa)	km^2	8.80
	Average slip(Da)	cm	50.0
	Seismic moment(M_{0a})	dyne・cm	1.41E+24
	Stress drop($\Delta\sigma$)	bar	140.9
Background	Area(Sb)	km^2	31.20
	Average slip(Db)	cm	17.9
	Seismic moment(M_{0b})	dyne・cm	1.79E+24
	Stress drop($\sigma b=\Delta\sigma\times 0.2$)	bar	28.2

The source parameter was shown in Table 2. Fault width and depth of fault top were equalized to the dynamic simulation. Fault length accorded with the length of rupture area in the dynamic simulation shown in Fig. 6. Other parameters were set based on Strong ground motion prediction method for earthquakes with

specified source faults ("Recipe") [8]. Average slip by "Recipe" was almost corresponding to the slip of the dynamic simulation shown in Fig. 9 and Fig. 10. Rupture velocity shown in Table 2 was the intermediate value between 1.5km/s and 3.5km/s shown in Fig. 7.

4.2 Predicted ground motions

Fig.13 shows velocity waveform on ground surface (z=0km) at 0.1km in y-direction apart from the fault line for the model with SMGA locating at the center of the fault. Y-component ground velocity was especially large around x=±1～5km.

On the other hand, Fig.14 shows velocity waveform for the model with SMGA locating at the boundary of media. Y-component ground velocity was especially large around x=±5～10km. This feature coincided with the result of the dynamic simulation. This coincidence implied that the SMGA didn't necessarily correspond to the large slip area.

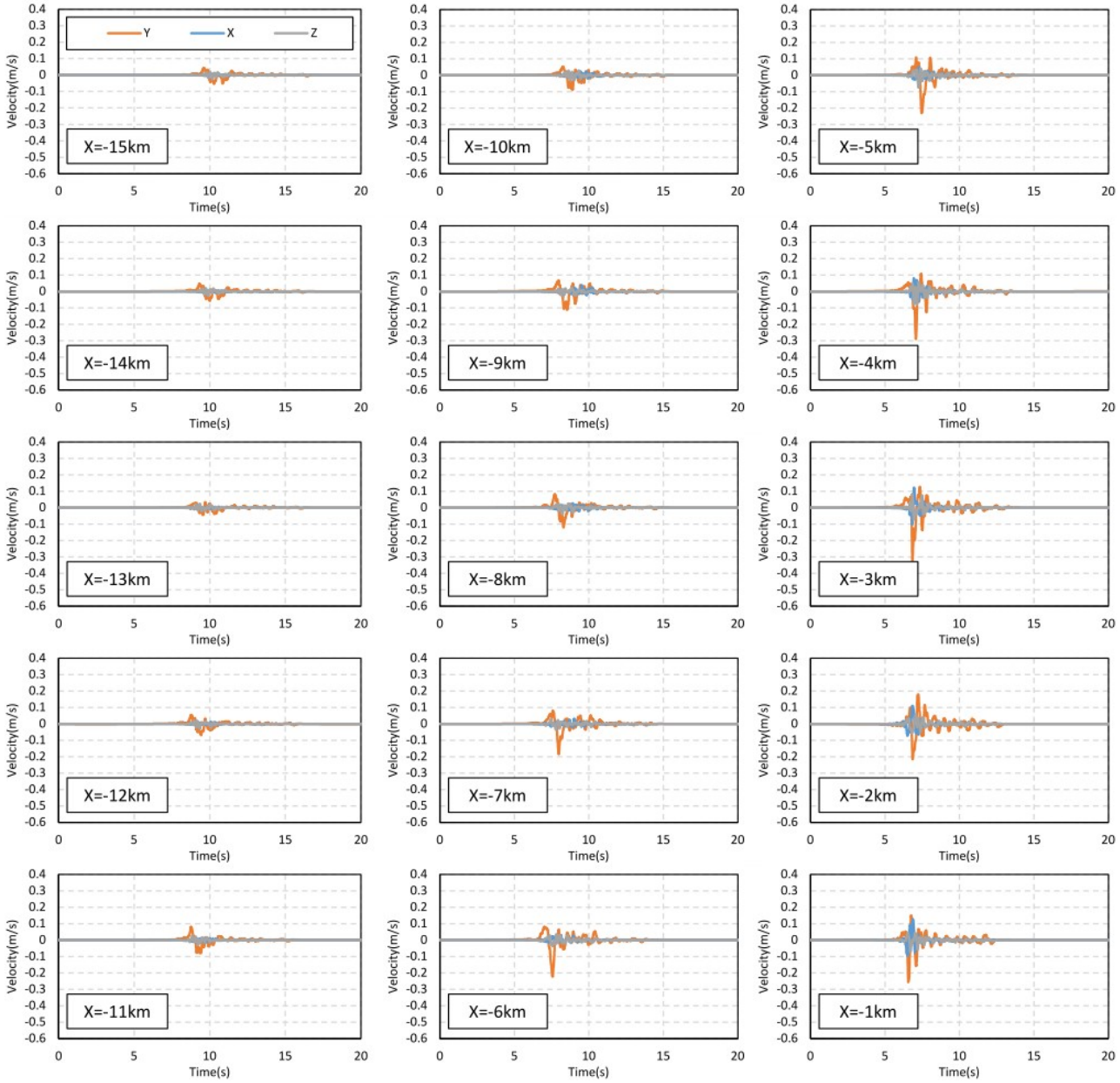

Fig. 13 – Predicted ground motion for model with SMGA locating at the center of the fault

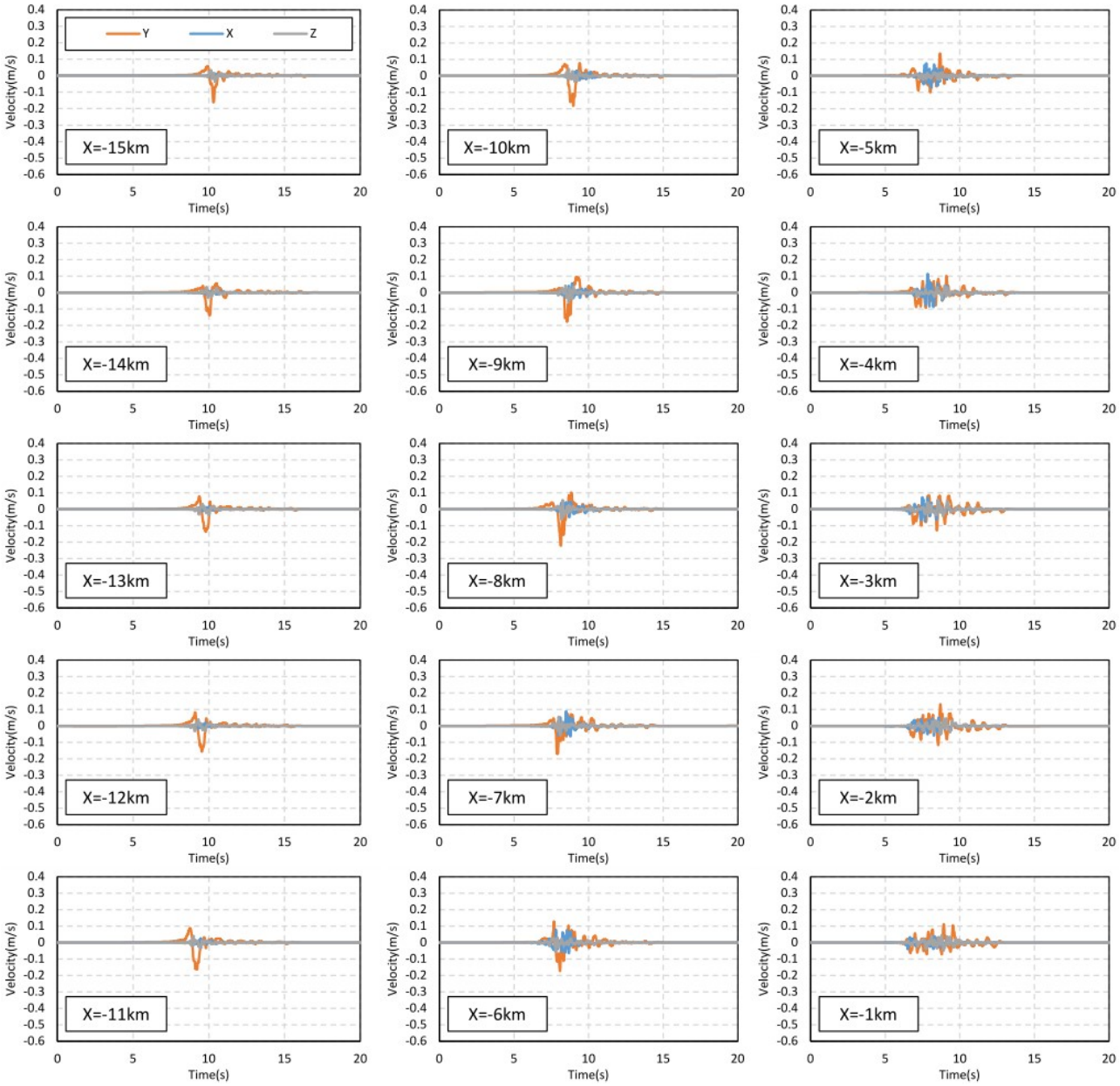

Fig. 14 – Predicted ground motion for model with SMGA locating at the boundary of media

5. Conclusion

The dynamic fault rupture simulation was conducted using the three dimensional finite difference method without giving a priori rupture starting area and rupture stopping area by changing the coefficient of friction or changing the frictional constitutive law. It was conducted on condition that the shear rigidity was changed along the fault plane and that the shear stress on the fault plane was loaded by forced dis-placement.

In this study, induced shear stress in the fault layer by the forced displacement was larger at the center part because of higher shear wave velocity and stress was smaller at the outskirts part because of lower shear wave velocity. The ununiform shear stress distribution caused that fault rupture spontaneously starting from the central part in spite of constant frictional condition in this layer. The fault rupture was spontaneously stopped after the rupture spread up to around 10km in the x-direction without giving a priori rupture stopping area by frictional condition.

It was consistent with previous studies in the fault rupture process that the rupture velocity was 3～3.5km/s at most. It was not incompatible with previous studies that the stress drop was about 2MPa. We could estimate the near fault ground motion for our model fault by using this dynamic rupture simulation. The slip velocity time function directly calculated by the dynamic fault rupture simulation was consistent with previous study.

Kinematic source models were prepared referring to the dynamic fault rupture simulation. The predicted ground motions by statistical Green's function method were compared with the motion predicted by the dynamic simulation. Y-component ground velocity was especially large around x=±5～10km for the model with SMGA locating at the boundary of media. This feature coincided with the result of the dynamic simulation. This coincidence implied that the SMGA didn't necessarily correspond to the large slip area.

We intend to conduct this dynamic fault rupture simulation for the more realistic model with which the actual conditions and properties of underground can be illustrated such as model size, stress condition, friction coefficient and so on.

6. References

[1] Tsuda K (2016): Dynamic Rupture Simulations Constrained by Experimental Data to Understand the Rupture Process of Mega-Thrust Earthquakes, Technical research report of Shimizu Construction Co., Ltd. 93: 82-88.

[2] Kase Y (2016): Dynamic rupture model of the 2014 northern Nagano, central Japan, earthquake (Part 3), Japan Geoscience Union meeting.

[3] Kase Y & Horikawa H & Sekiguchi H & Satake K & Sugiyama Y (2002): Simulation of earthquake rupture process on the Uemachi fault system, Annual report on active fault and paleoearthquake researches 2: 325-340.

[4] Irie K (2014): Source properties of inland strike-slip faults for strong motion prediction based on dynamic rupture simulation, Doctoral thesis of Hirosaki University.

[5] Kame N (1997): Theoretical study on arresting mechanism of dynamic earthquake faulting -A new method of the analysis of spontaneous rupture growth with geometrical complexity, D. Sc. Thesis, the University of Tokyo.

[6] Kase Y (2010): Slip-length scaling low for strike-slip multiple segment earthquakes based on dynamic rupture simulations, Bulletin of the Seismological Society of America 100(2): 473-481.

[7] Nakamura H & Miyatake T (2000): An approximate expression of slip velocity time function for simulation of near-field strong ground motion, Zisin2 53: 1-9.

[8] The Headquarters for Earthquake Research Promotion (2017): Strong ground motion prediction method for earthquakes with specified source faults. ("Recipe").

